Searching for MeV-scale Axion-like Particles and Dark Photons with PandaX-4T

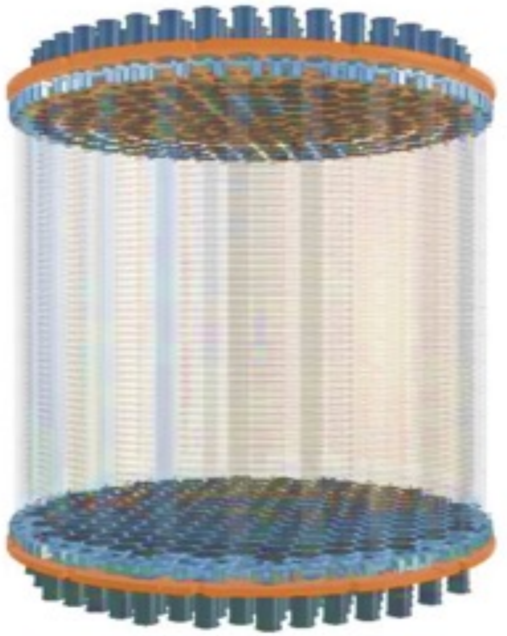

Tao Li (李涛)

On behalf of the PandaX Collaboration

PANDA X
PARTICLE AND ASTROPHYSICAL XENON TPC

TAUP XICHANG

TAUP2025

27th Aug. 2025

上海交通大學
SHANGHAI JIAO TONG UNIVERSITY

taoli@sjtu.edu.cn

Light Bosonic Dark Matter: ALPs and DPs

- **No positive results of WIMP motivate various theoretical models of low-mass dark matter.**
- **Axion-like particles (ALPs)**
  - **Pseudoscalar bosons**, non-thermally produced via the misalignment mechanism,
  - Provide the necessary abundance of light cold dark matter.
  - Interact with SM particles through the **axioelectric effect** (similar to the photoelectric effect).

$$\sigma_{ae} = \sigma_{pe} \frac{g_{ae}^2}{\beta} \frac{3E^2}{16\pi\alpha m_e^2} \left(1 - \frac{\beta^{\frac{2}{3}}}{3}\right)$$

Absorbed by a detector's atom, which later releases an electron in the final state.

- Given that velocity of DM is 0.001c, and the local density is 0.3 GeV/cm^3:

$$R_{\mathrm{ALP}} = \frac{1.47 \times 10^{19}}{A} g_{ae}^2 \cdot m_a \sigma_{pe} \ \ [\mathrm{kg}^{-1}\mathrm{d}^{-1}]$$

Light Bosonic Dark Matter: ALPs and DPs

➢ Dark photons (DPs)

- **Vector bosons**, generated through inflationary perturbations.
- Weakly interact with photons through **kinetic mixing**.

$$\sigma_{\mathrm{DP}} = (e^2 c / 4\pi\alpha v) \cdot \kappa^2 \cdot \sigma_{pe}$$

$$R_{\mathrm{DP}} = \frac{4.7 \times 10^{23}}{A} \frac{(e\kappa)^2}{4\pi\alpha} \frac{\sigma_{pe}}{m_d} \quad [\mathrm{kg}^{-1}\mathrm{d}^{-1}]$$

➢ Experimental searches

XENONnT is leading the limit at the masses below 140 keV/c^2, while GERDA and COSINE-100 set in the 150 keV/c^2 to 1 MeV/c^2.

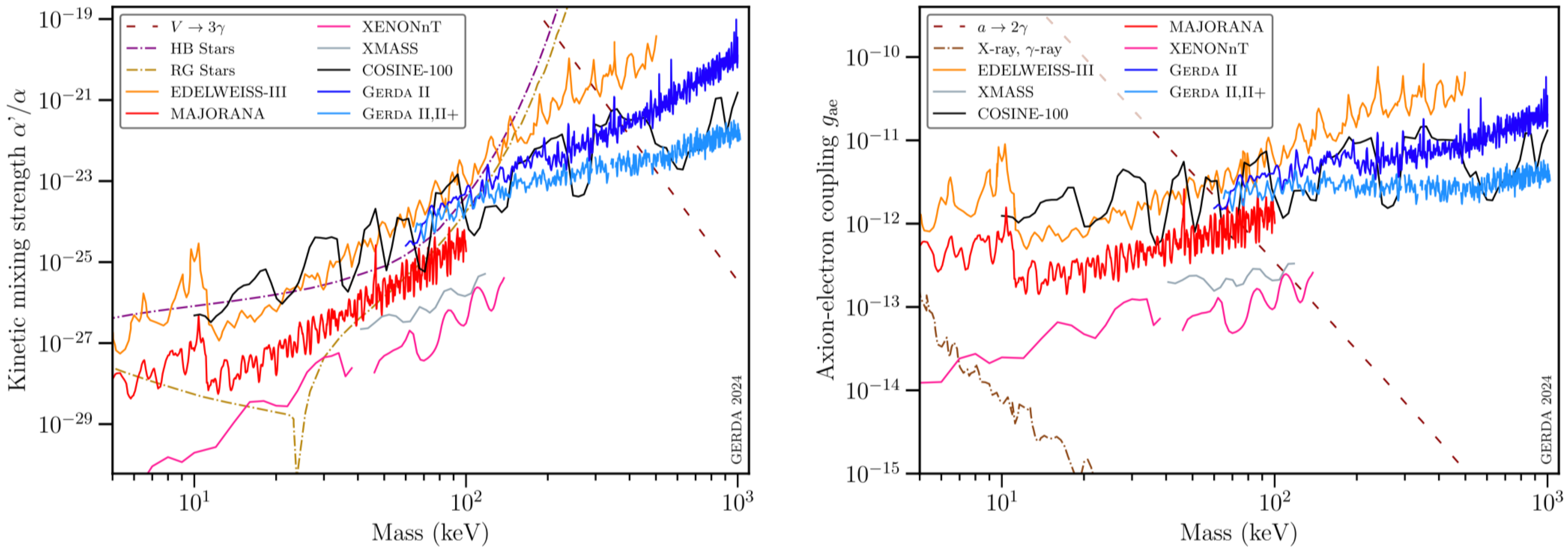

Eur. Phys. J. C 84, 940 (2024)

*** Only the absorption process is considered in our analysis.**

A dedicated analysis focused on MS events (Compton-like process) is underway.

PandaX - Particle and Astrophysical Xenon

- Dark matter direct detection, Majorana neutrinos, and astrophysical neutrinos.

16 institutions, ~ 100 collaborators

PandaX-4T Detector

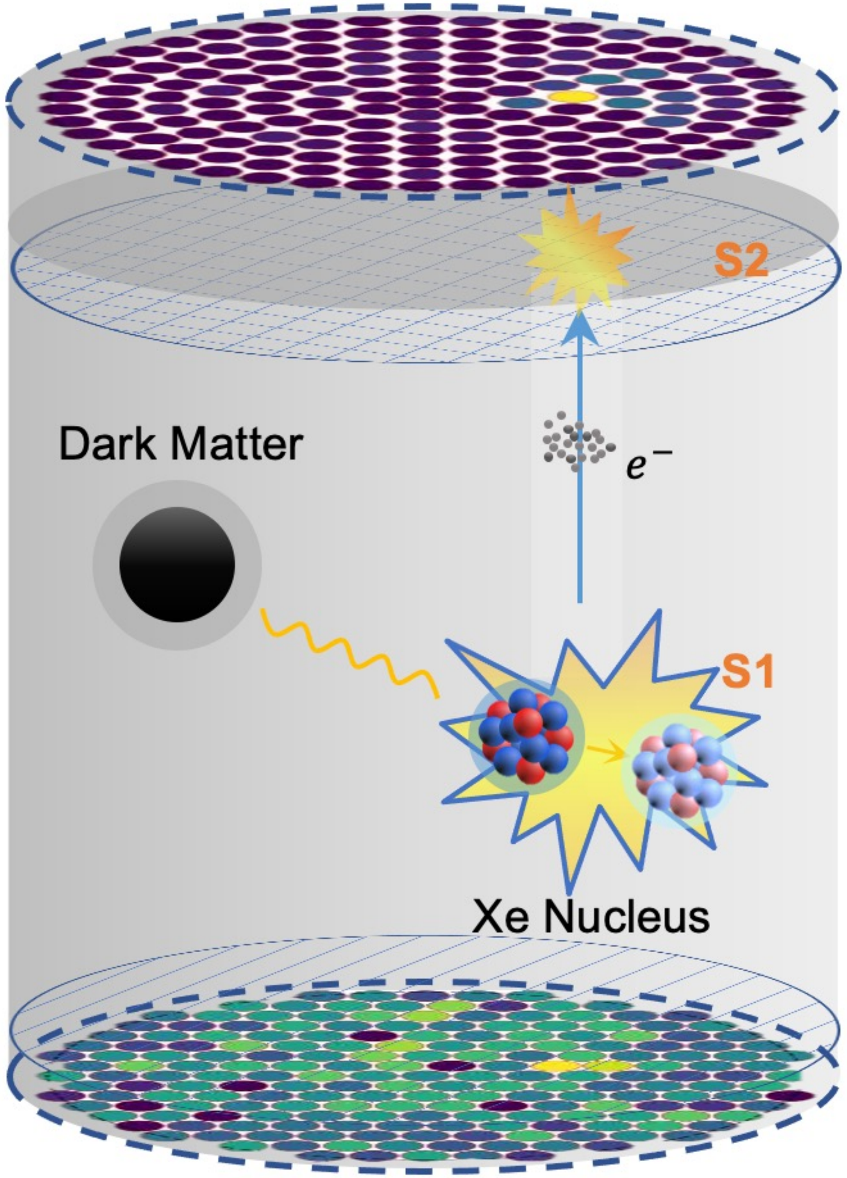

- Located at CJPL-II;
- Dual-phase Xe TPC: 3.7-ton natural LXe;
- 3-inch PMTs array: 169 top / 199 bottom;
- Primary scintillation signal (S1); Electroluminescence signal (S2);
- Precise energy, 3D position measurement.

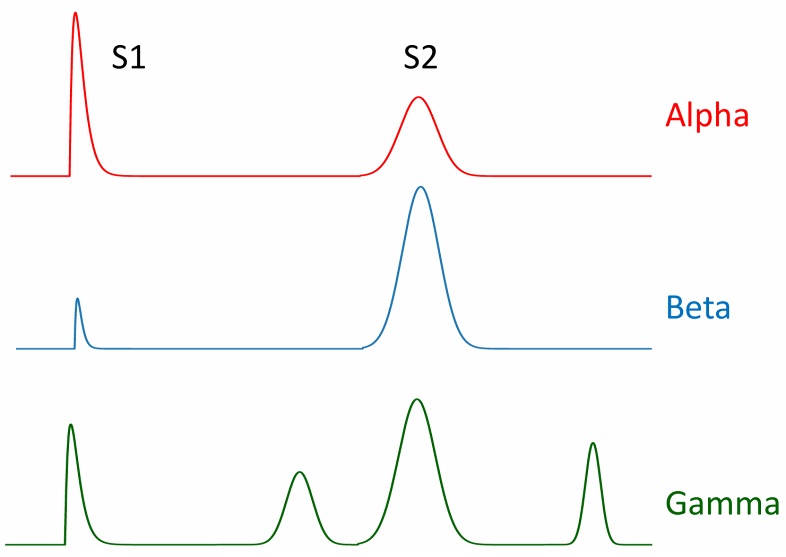

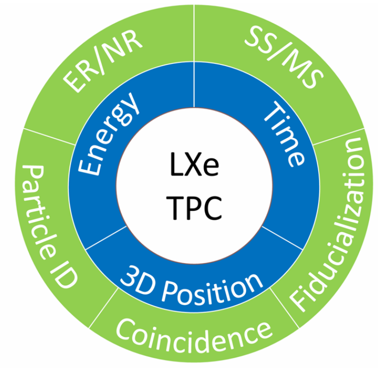

PandaX-4T Physics Run

2020/11 – 2021/04	**Commissioning (Run0)** 95 days
2021/07 – 2021/10	**Tritium removal** xenon distillation, gas flushing, etc
2021/11 – 2022/05	**Physics run (Run1)** 164 days
2022/09 – 2023/12	**CJPL B2 hall construction** xenon recuperation, detector upgrade
Current Status	**Physics run (Run2)**

Phys.Rev.Lett. 134, 011805 (2025)
(Details seen in the next talk)

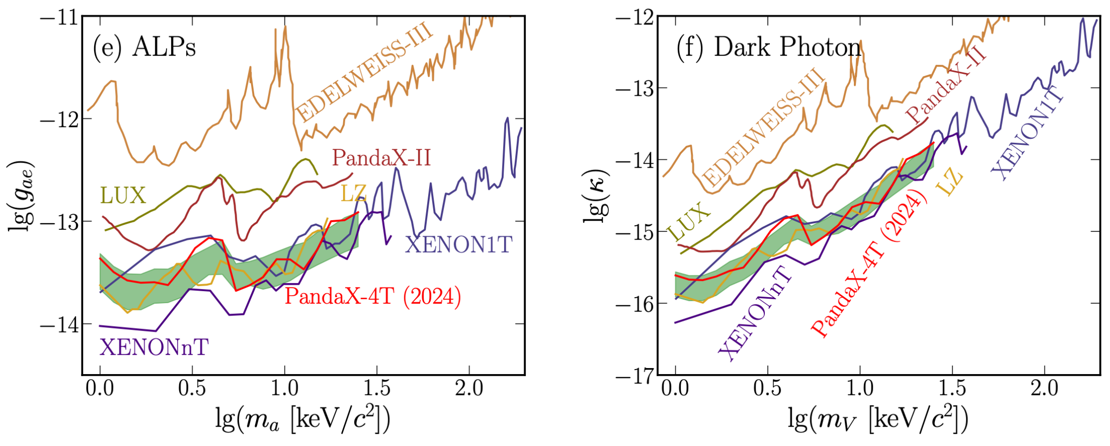

Energy Region Extension

- Severe **waveform saturation** in the MeV range in Run0+1, while it has been solved by the updated base design in Run2.
- Waveform matching method to restore the gradient information.

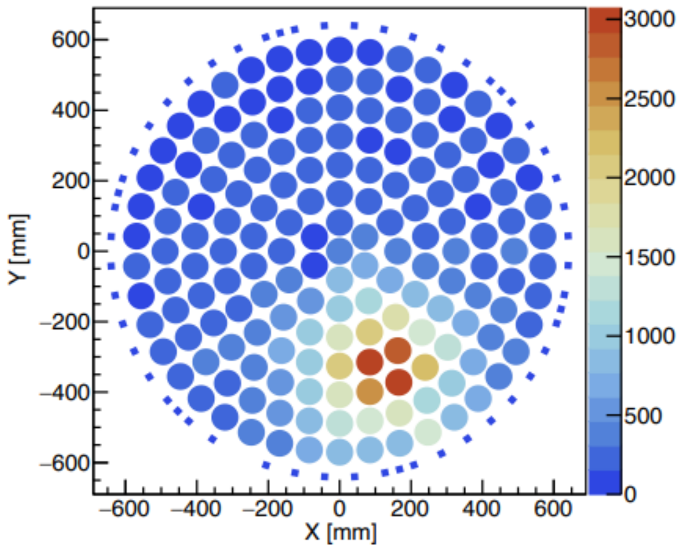

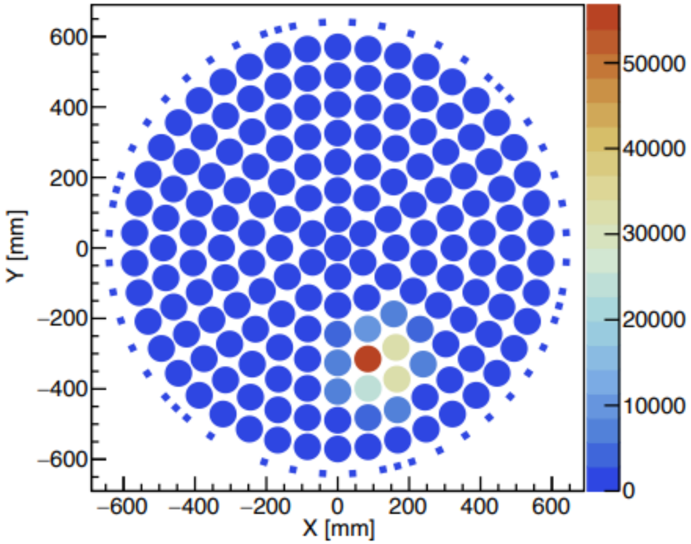

Baseline design for PandaX-4T

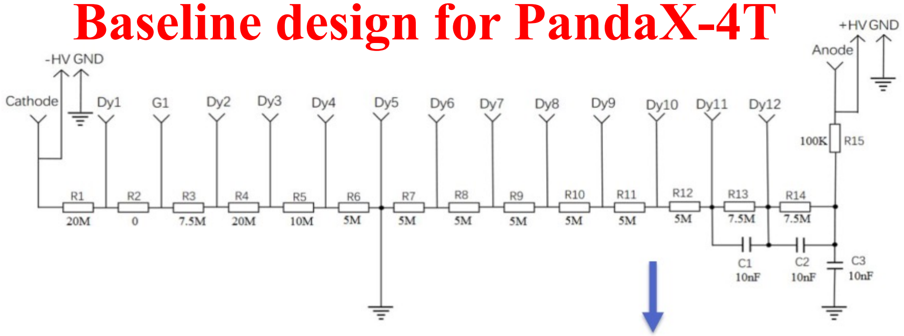

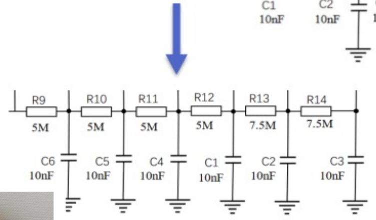

Updated design

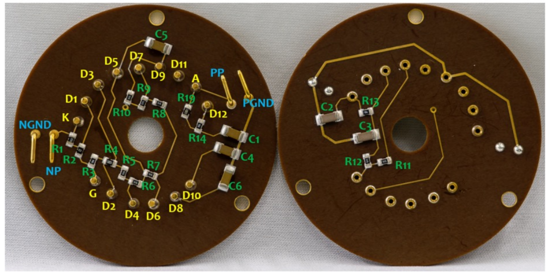

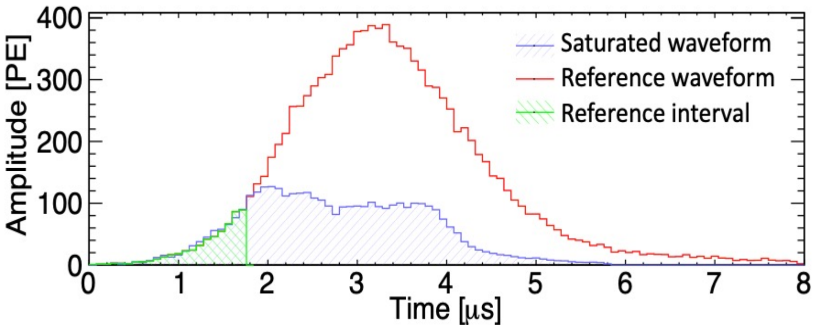

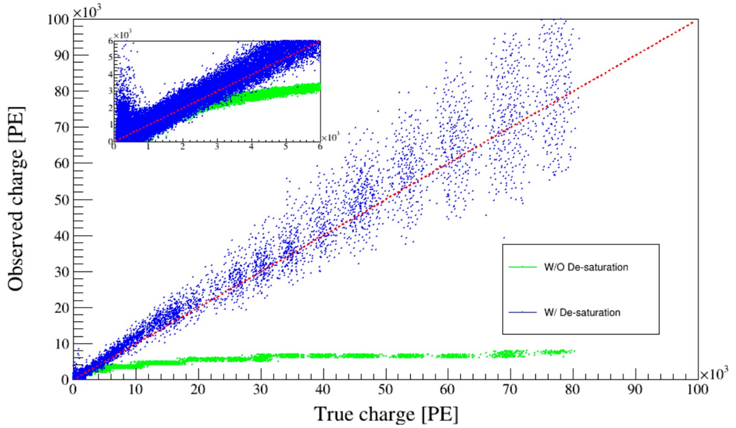

Energy Reconstruction

➢ Energy reconstruction:

$$E = 13.7\ \text{eV} \times \left(\frac{S1}{\text{PDE}} + \frac{S2_B}{\text{EEE} \times \text{SEG}_\text{B}} \right)$$

- **PDE**: photon detection efficiency for $S1$;
- **EEE**: electron extraction efficiency;
- **SEG$_\text{B}$**: single-electron gain for $S2$;

- Due to the dead channels and saturation of the top PMTs, ***$S2_B$*** is used.
- **Non-uniformity** of detector response is corrected in three dimensions by ^{83m}Kr calibration data (41.5 keV);
- Energy calibration from γ peaks (41.5 keV, 164 keV, 236 keV, 1460 keV);

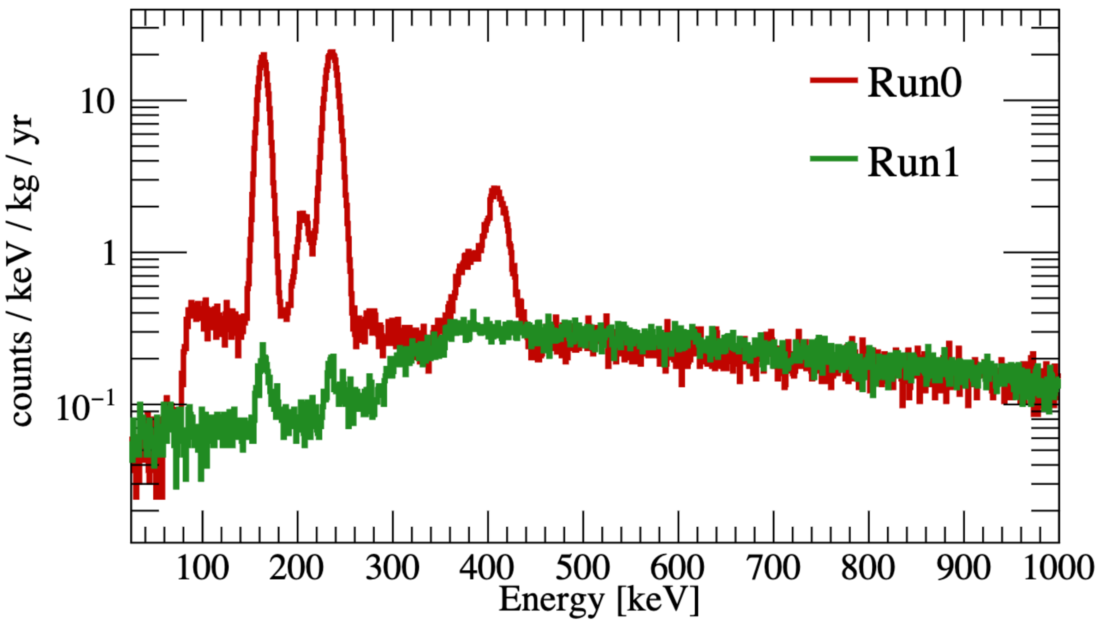

Energy Reconstruction

➢ Energy response model:

- **Energy resolution**: $\frac{\sigma(E)}{E} = \frac{a}{\sqrt{E}} + b \cdot E + c$
- **Energy scale**: $E = d \cdot \hat{E} + e$
- Calibrated by multiple mono-energetic peaks during dedicated calibration periods or physics runs.
- The reconstructed spectrum is a convolution of the true energy spectrum.
- The expected values $\mathcal{M}_0 = (a_0, b_0, c_0, d_0, e_0)^T$, with a 5x5 covariance matrix Σ_m.

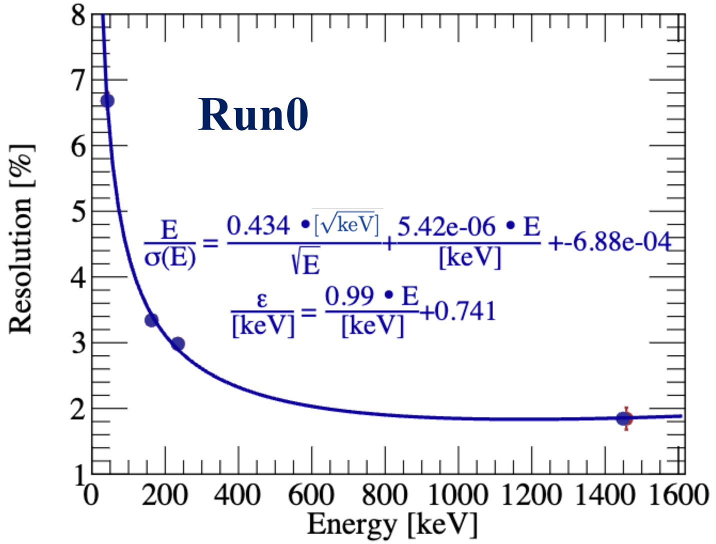

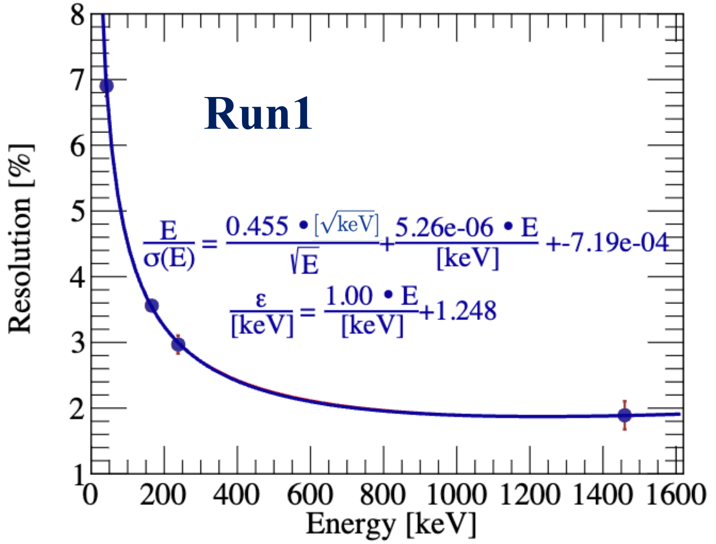

Fiducial volume (FV) and exposure

- **The same FV is used in ^{136}Xe DBD analysis.**
  - Confirmed for a high signal-to-noise ratio.
  - **625 (621) kg** natural xenon within the FV;
  - **94.8 (163.5) live days** of data from the initial data release;

Total exposure:
440 kg·yr (Run0 + Run1)

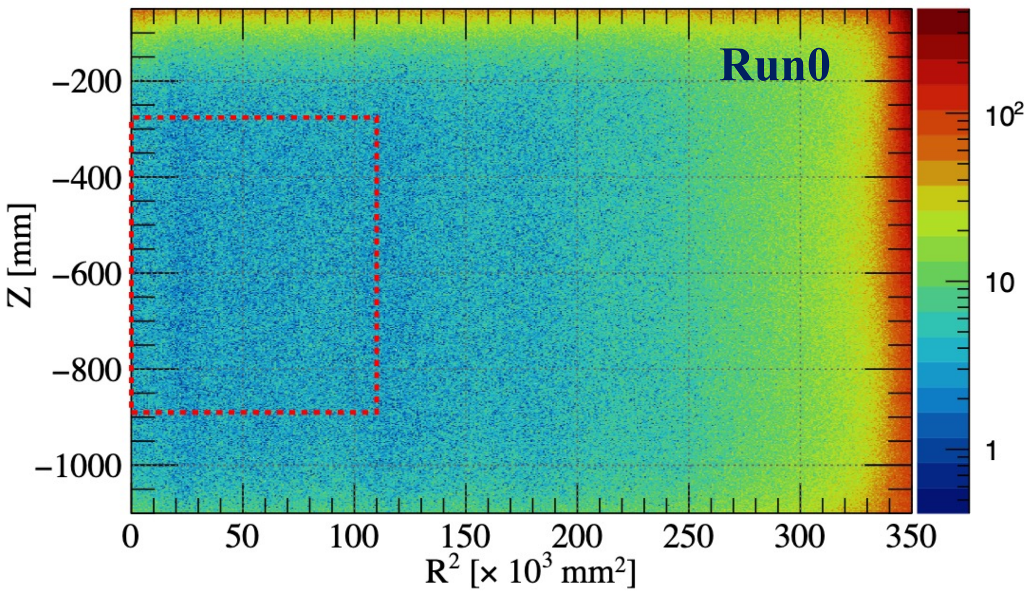

- **Target mass uncertainty:**
  - Density of LXe (0.14% for Run0 and Run1);
  - FV selection (Run0: 1.6%, Run1: 2.1%);

The difference between the geometrically calculated by ^{83m}Kr Calibration data.

Background model

1. **Detector materials: ^{60}Co, ^{40}K, ^{232}Th, ^{238}U**
   - Expected radioactivity from the HPGe Station.
   - Apply the **biasing** technology in the Monte-Carlo simulation.
2. **solar neutrino (*pp* + ^{7}Be)**
   - A many-body calculations for the structure, photoionization , and the neutrino-ionization of xenon. ***Phys.Lett.B* 774 (2017) 656-661**
3. **liquid Xenon**

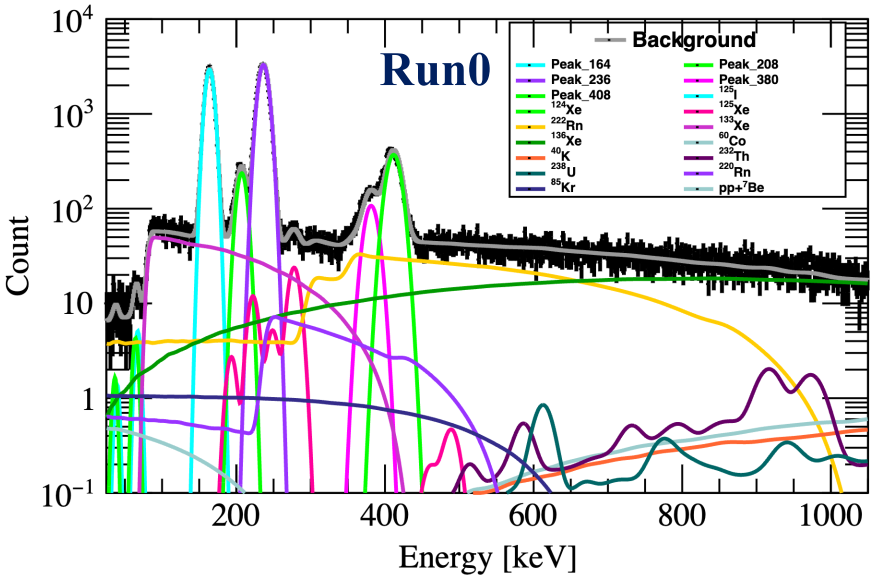

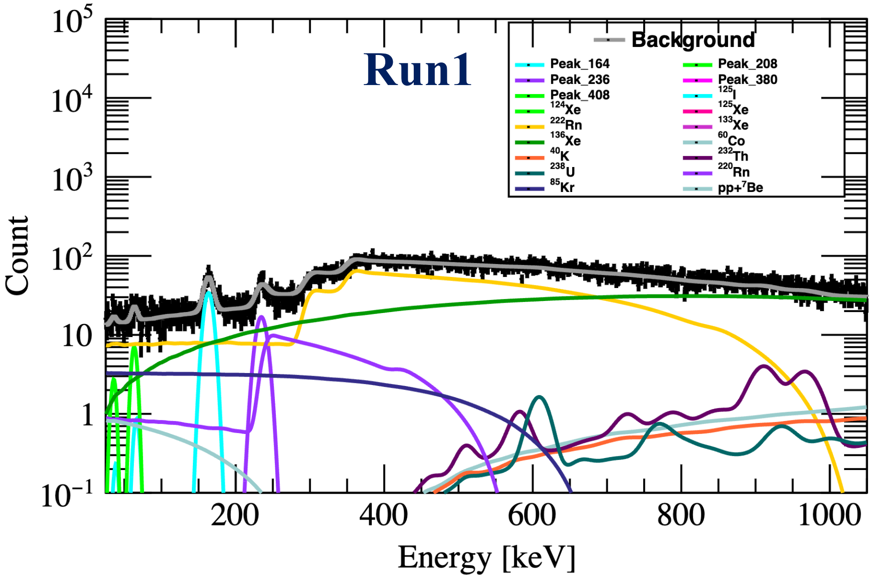

Components	Expected ($\times 10^2$)
^{232}Th	9.7 ± 5.8
^{238}U	3.8 ± 2.8
^{60}Co	5.8 ± 3.5
^{40}K	4.5 ± 2.0
^{85}Kr	19.0 ± 4.9
^{214}Pb	float
^{212}Pb	float
^{136}Xe	352 ± 16
^{124}Xe	1.37 ± 0.21
^{125}Xe (Run0)	float
^{125}I	0.66 ± 0.16
^{133}Xe (Run0)	float
164 keV (Run0)	414 ± 17
164 keV (Run1)	float
208 keV (Run0)	37.8 ± 1.3
236 keV (Run0)	565 ± 66
236 keV (Run1)	float
380 keV (Run0)	24.3 ± 1.2
408 keV (Run0)	87.9 ± 3.2
pp+^{7}Be ν	2.22 ± 0.24

Background model

- **Biasing technology for material background**
  1. Split the sensitive volume;
  2. Record "bias_hit" and "bias_source";
  3. Generate the event by the "bias_source" from the previous run and increase the simulated numbers;
  4. Combine "bias_hit";
     - **"bias_hit":** Energy deposition;
     - **"bias_source":** The information of particles that touch the inner boundary.

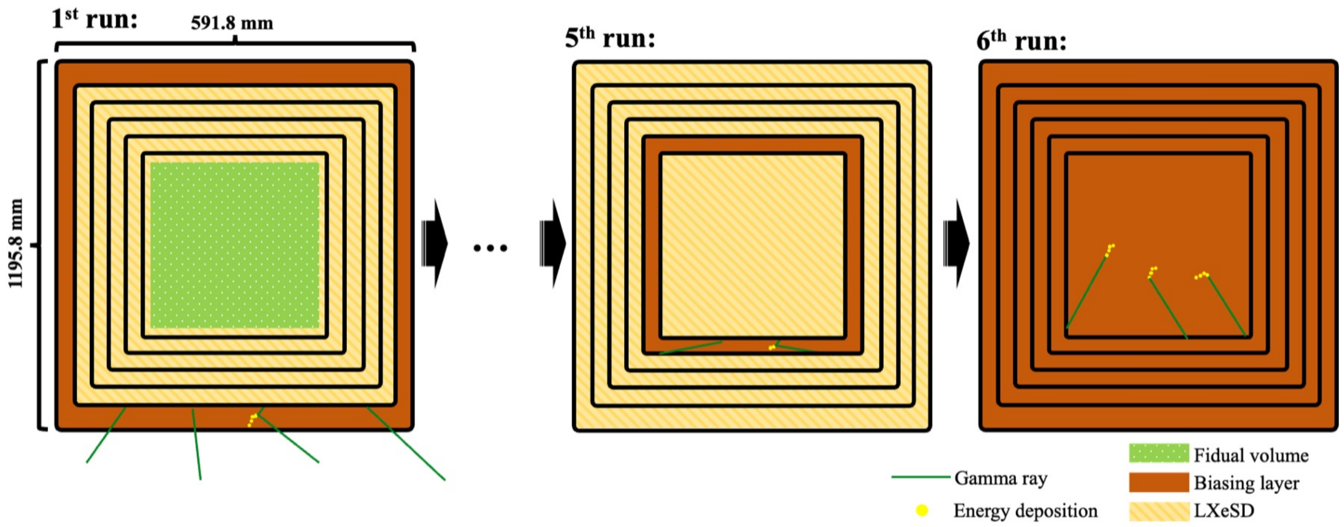

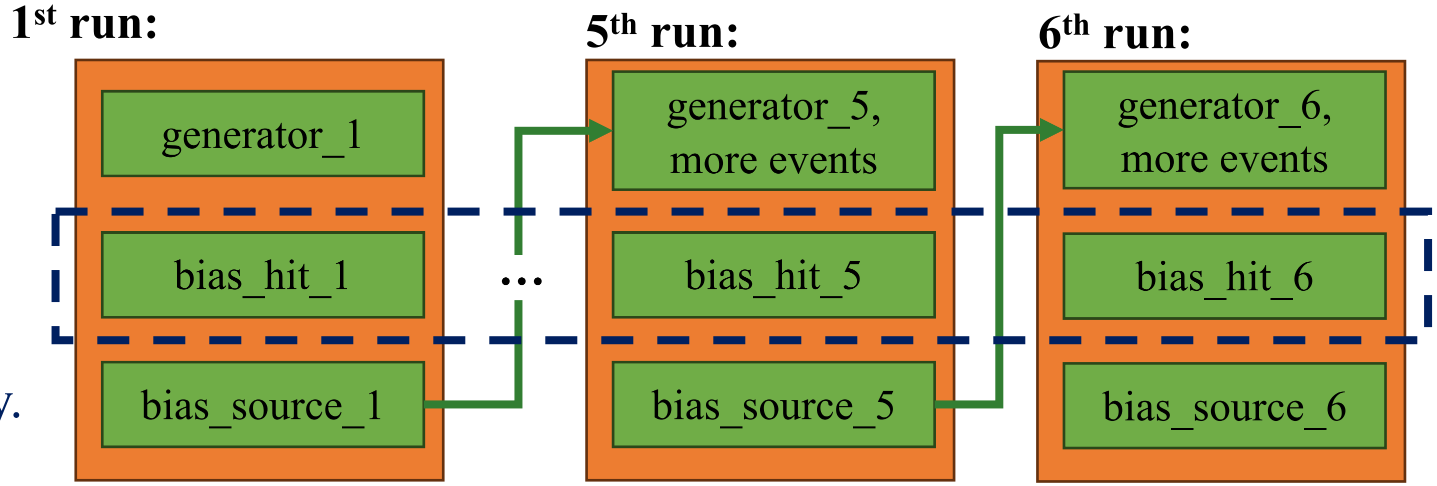

By reusing the results of previous layers, more statistics can be achieved in less time.

Background model

3. Liquid Xenon:

- ^{136}Xe DBD, ^{124}Xe double electron capture, ^{125}I, ^{85}Kr ;
- ^{125}Xe, ^{133}Xe, ^{214}Pb: float;
- ^{212}Pb: float due to the strong dependence on the circulation conditions.
- **^{127}Xe** (30 kg of xenon from above-ground in Run0),
- **^{129m}Xe and ^{131m}Xe** (neutron calibration during and after Run0).

First estimated in PandaX-4T.

Gaussian peaks	
164 keV	^{131m}Xe gamma(IC)
208 keV	L-shell EC + ^{127}I 203 keV gamma
236 keV	K-shell EC + ^{127}I 203 keV gamma ^{129m}Xe 196.6 keV + 39.6 keV(IC)
380 keV	L-shell EC + ^{127}I 375 keV gamma
408 keV	K-shell EC + ^{127}I 375 keV gamma

Half-lives [day]	
^{129m}Xe	8.88
^{131m}Xe	11.8
^{127}Xe	36.4

Components	Expected
^{85}Kr	19.0 ± 4.9
^{214}Pb	float
^{212}Pb	float
^{136}Xe	352 ± 16
^{124}Xe	1.37 ± 0.21
^{125}Xe (Run0)	float
^{125}I	0.66 ± 0.16
^{133}Xe (Run0)	float
164 keV (Run0)	414 ± 17
164 keV (Run1)	float
208 keV (Run0)	37.8 ± 1.3
236 keV (Run0)	565 ± 66
236 keV (Run1)	float
380 keV (Run0)	24.3 ± 1.2
408 keV (Run0)	87.9 ± 3.2

Gaussian peaks should be treated carefully, affecting the fit with similar signal energy.

Background model

➢ Time evolution of ^{127}Xe, ^{129m}Xe and ^{131m}Xe in Run0

- A larger FV for increasing statistics (2.4 tons);
- Characterize with a Gaussian + linear function for each Gaussian component;
- The measured half-lives of these xenon isotopes agree with the expected values.

Components	Expected
164 keV (Run0)	414 ± 17
164 keV (Run1)	float
208 keV (Run0)	37.8 ± 1.3
236 keV (Run0)	565 ± 66
236 keV (Run1)	float
380 keV (Run0)	24.3 ± 1.2
408 keV (Run0)	87.9 ± 3.2

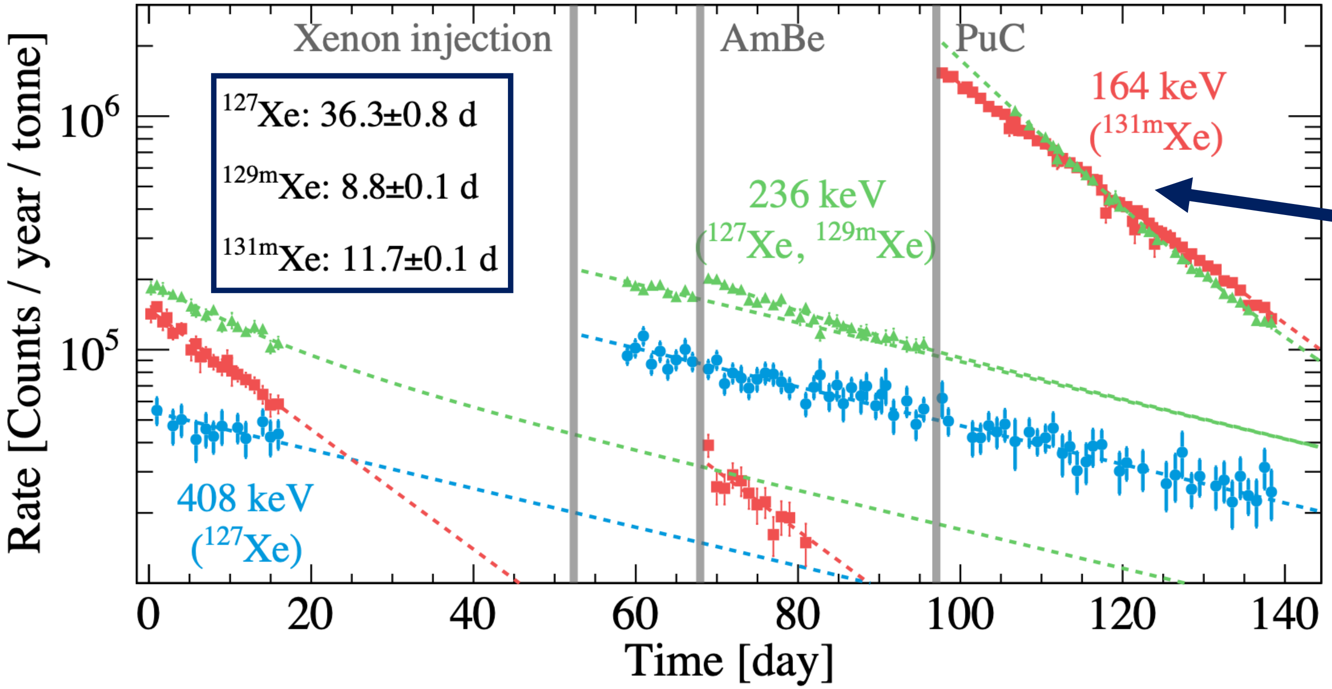

Xe131m: run3641

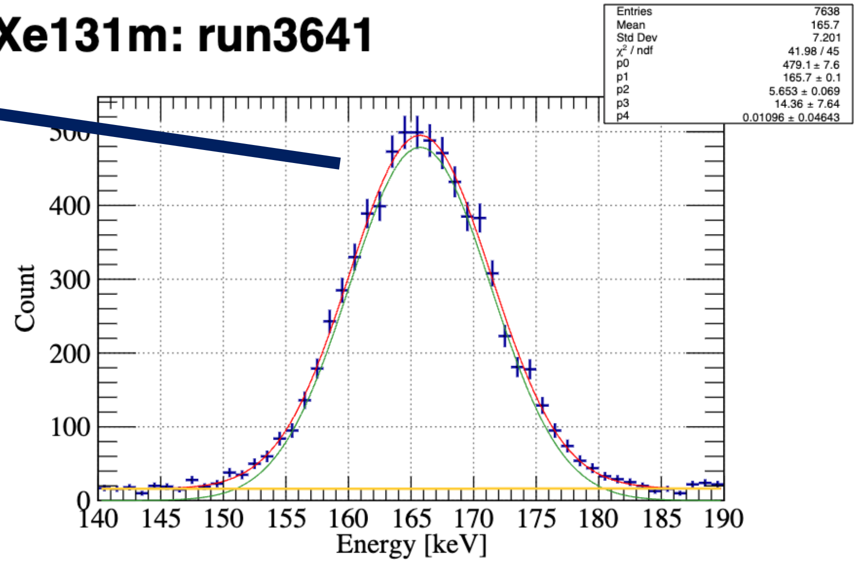

Binned likelihood method

➢ Likelihood definition

$$L = \prod_{r=0}^{1} \prod_{i=1}^{N_{\text{bins}}} \frac{(N_{r,i})^{N_{r,i}^{\text{obs}}} e^{-N_{r,i}}}{N_{r,i}^{\text{obs}}!} \mathcal{G}(\mathcal{M}_r; \mathcal{M}_r^0, \Sigma_r) \cdot \prod_{j=1}^{N_G} G(\eta_j; 0, \sigma_j)$$

Detector response

Nuisance parameters

Overall efficiency **Signal selection** **Background model**

$$N_i = (1+\eta_a) \cdot [(1+\eta_s) \cdot n_s \cdot S_i + \sum_{b=1}^{N_{\text{bkg}}} (1+\eta_t) \cdot n_b \cdot B_{b,i}]$$

- N_i, N_i^{obs}: expected and observed numbers of events in the i_{th} energy bin;
- n_s, n_b: the counts of signal s and background component b;
- S_i, $B_{b,i}$: the i_{th} bin values of the normalized energy spectrum **convolved with the five-parameter energy response model**;

Systematic uncertainties:

	Sources	Run0	Run1
Detector response	a_0 [$\sqrt{\text{keV}}$]	0.43 ± 0.02	0.45 ± 0.02
	b_0 [keV^{-1}]	$(5 \pm 2) \times 10^{-6}$	$(5 \pm 2) \times 10^{-6}$
	c_0	$(-7 \pm 20) \times 10^{-4}$	$(-7 \pm 22) \times 10^{-4}$
	d_0	0.9930 ± 0.0008	0.9989 ± 0.0009
	e_0 [keV]	0.74 ± 0.06	1.25 ± 0.06
Overall efficiency	SS fraction (1 MeV/c^2)	$(96 \pm 4)\%$	$(96 \pm 4)\%$
	Quality cut	$(99.87 \pm 0.02)\%$	$(99.75 \pm 0.10)\%$
Signal selection	LXe density [g/cm^3]	2.850 ± 0.004	
	FV uniformity [kg]	625 ± 10	621 ± 13
Background model			

Limits on coupling constant

- Raster scan for hypothetical Gaussian peaks in **[30 keV/c², 1 MeV/c²]** with **10 keV/c²** per step.
- The global significance is **1.5 σ**. No signal excess over background expectations is observed.
- The upper limits on the event rate at 90% C.L. are set and converted to the upper limits of coupling strength:

$$R_{\mathrm{ALP}} = \frac{1.2 \times 10^{19}}{A} g_{ae}^2 \cdot m_a \sigma_{pe} \ [\mathrm{kg}^{-1}\mathrm{d}^{-1}]$$

$$R_{\mathrm{DP}} = \frac{4 \times 10^{23}}{A} \frac{(e\kappa)^2}{4\pi\alpha} \frac{\sigma_{pe}}{m_d} \ [\mathrm{kg}^{-1}\mathrm{d}^{-1}],$$

The most competitive limits almost range from 150 keV/c² to 1 MeV/c², with an average improvement of 2.0 times better.

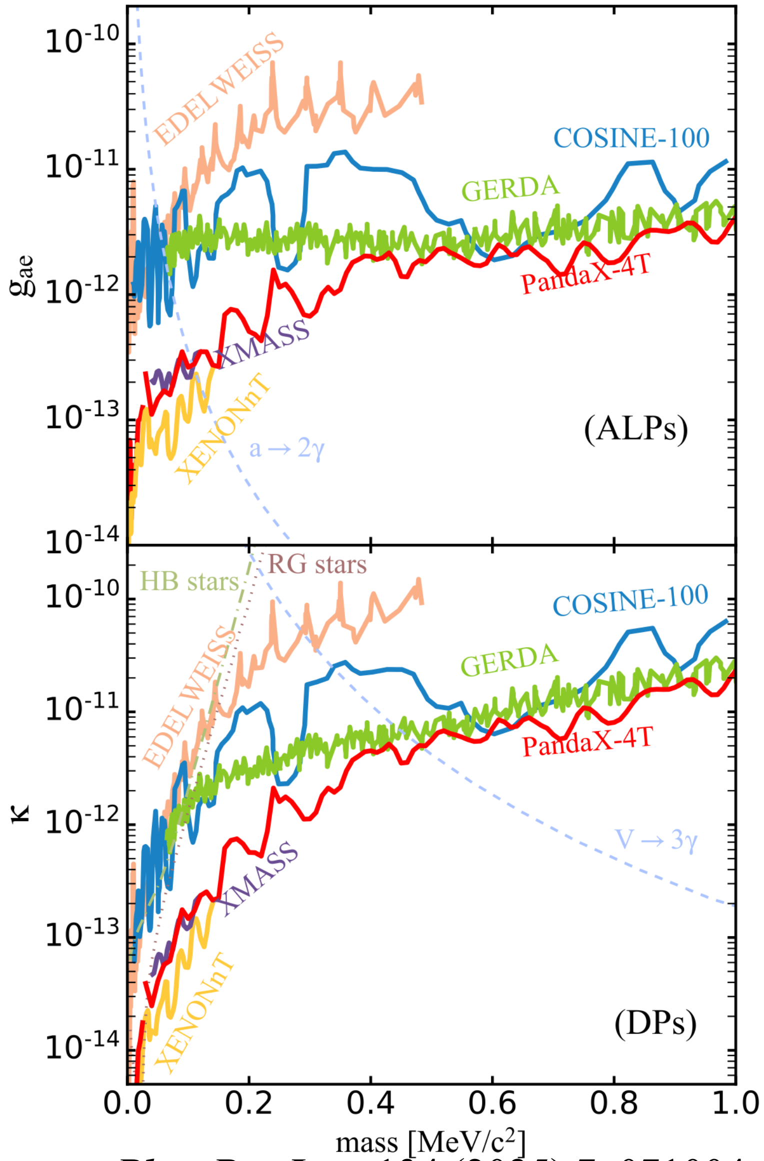

Phys.Rev.Lett. 134 (2025) 7, 071004

Summary

- We searched for ALPs and DPs with masses up to 1 MeV/c^2 using 440 kg yr exposure of PandaX's physical dataset.
  - A detailed analysis of the time evolution of xenon isotopes and the biasing technology improve the background modeling.
  - Including energy response model convolution in the likelihood function results in a more rigorous treatment of systematic uncertainties.
- No significant excess and most competitive limits in [150 keV/c^2, 1 MeV/c^2], due to a combination of large exposure, low background rate, and broader energy range.

Thank you for listening~

Searching for MeV-scale Axion-like Particles and Dark Photons with PandaX-4T

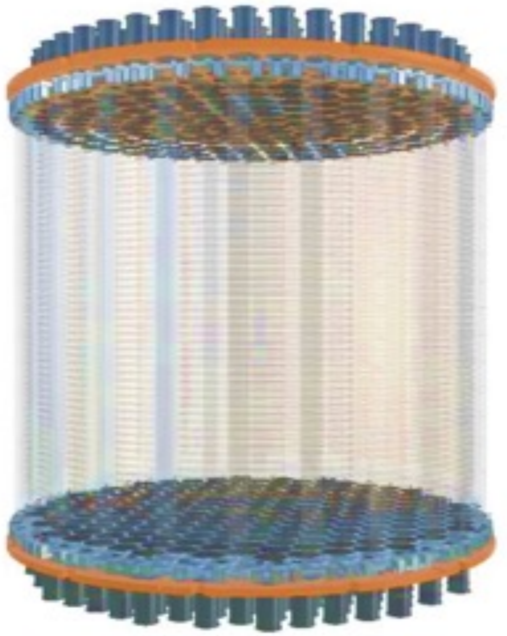

Tao Li (李涛)

On behalf of the PandaX Collaboration

TAUP XICHANG

TAUP2025

27th Aug. 2025

PANDA X

PARTICLE AND ASTROPHYSICAL XENON TPC

上海交通大學

SHANGHAI JIAO TONG UNIVERSITY

taoli@sjtu.edu.cn

Outlook

- **MS?**

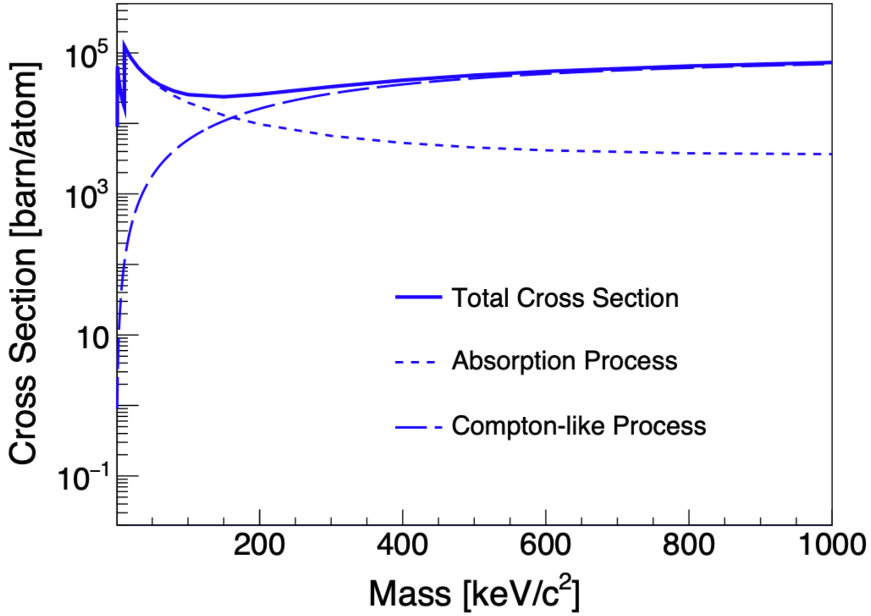

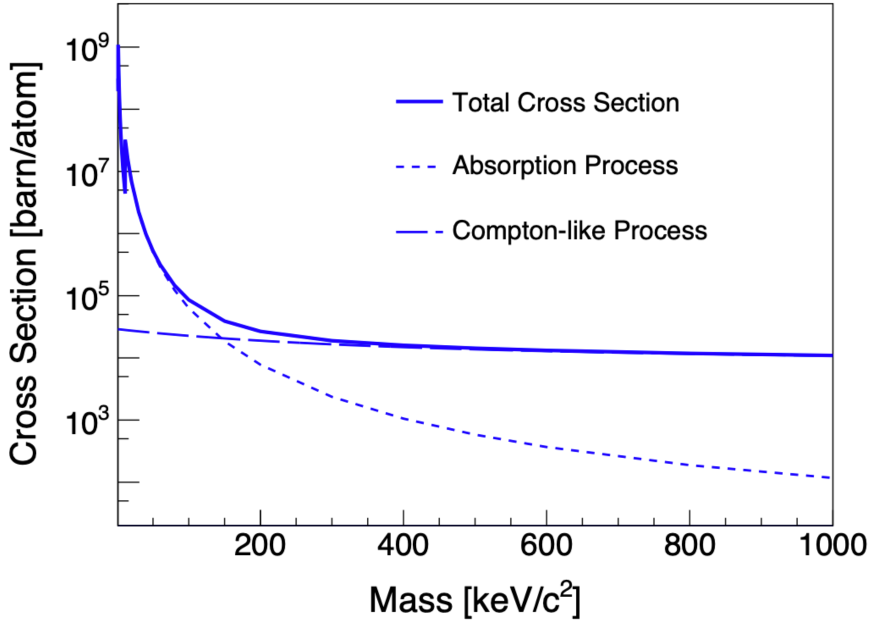

DM

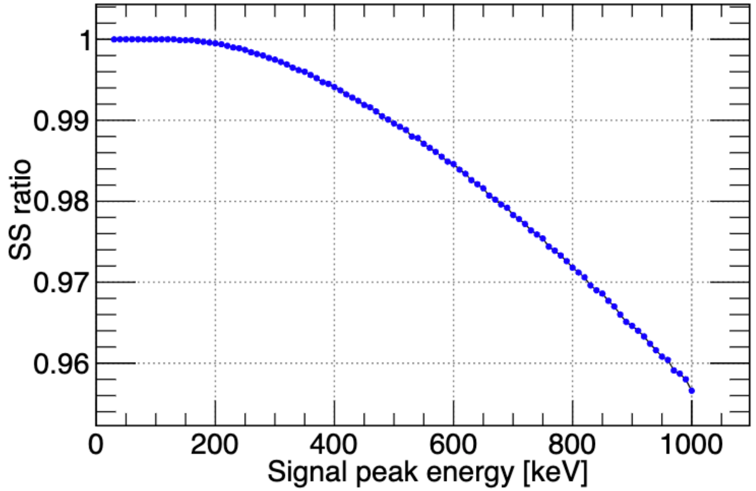

Searching for Signal in PandaX-4T

- **PandaX-4T has given the limits in [0, 30 keV/c^2], while the allowed mass region is from ~ keV/c^2 to 1 MeV/c^2.**

  (Details seen the next presentation)

- **In this report, we have searched for ALPs/DPs with masses up to 1 MeV/c^2 using the data of PandaX-4T Run0 and Run1.**

  1. **Energy region extension (near MeV region);**
  2. **Background model (mono-energetic compone);**
  3. **Systematics uncertainty (energy response);**

Multi-physics Targets

- Energy region from sub keV to several MeV.
- Region of Interest (ROI) here: [25 keV, 1MeV].

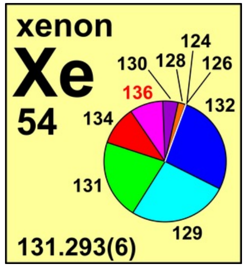

	sub keV	1keV	10 keV	100 keV	1MeV	10 MeV

^{136}Xe (~9%) — $2\nu\beta\beta/0\nu\beta\beta$

^{134}Xe (~10%) — $2\nu\beta\beta/0\nu\beta\beta$

^{124}Xe (~0.1%) — $2\nu DEC$

MeV region

Natural Xenon

WIMPs, boosted dark matter, ALPs, DPs, ...

Solar Axion

Solar pp ν

keV region

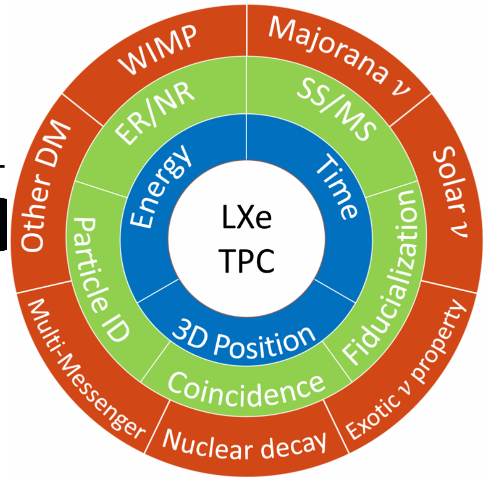

Signal in PandaX-4T detector

- monoenergetic peak related to the mass of ALP/DP, smeared by the response model.
- The mass points of ALP/DP are in [30 keV/c^2 , 1 MeV/c^2] with a step of 10 keV/c^2.
- ROI cut ([25, 1050] keV):

  efficiency ~100%

- SS ratio in ROI:

  Ranging from 100% to 95.7%

  based on Monte-Carlo simulation;

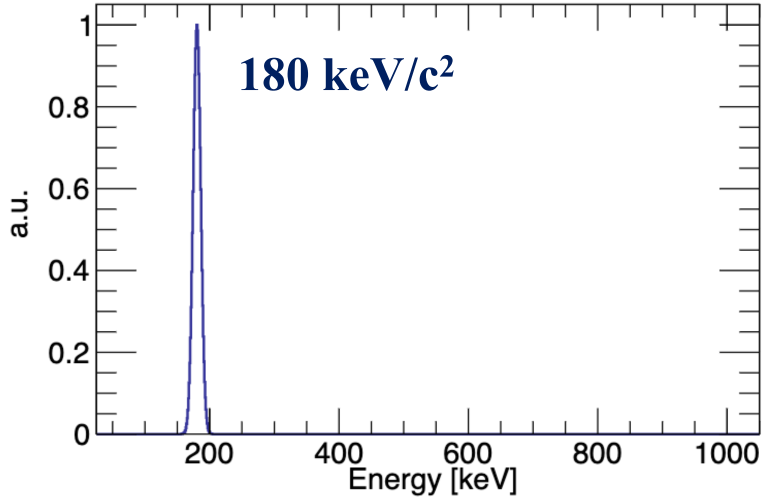

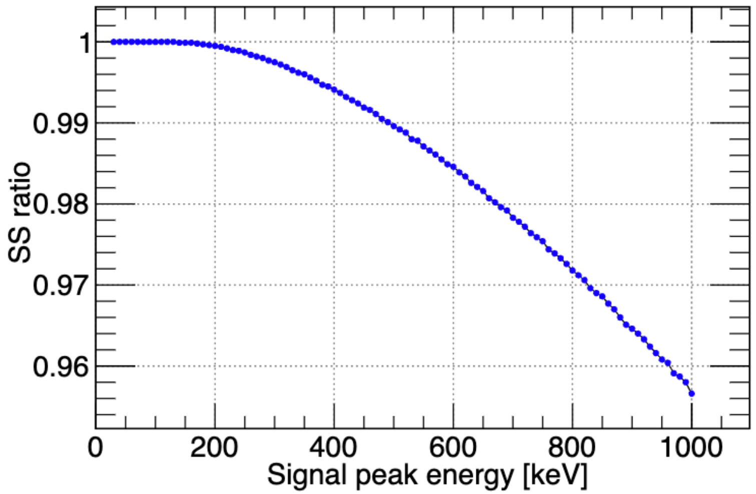

total detection efficiency = data quality cut efficiency × SS cut efficiency × ROI acceptance.

Event selection

➢ Data quality cuts efficiency:

Run0: (99.87 ± 0.02) %, Run1: (99.75 ± 0.10) %

- S1, S2, S1/S2: remove non-electron recoil and alpha events;
- Top and bottom S1 charge asymmetry vs. drift time;

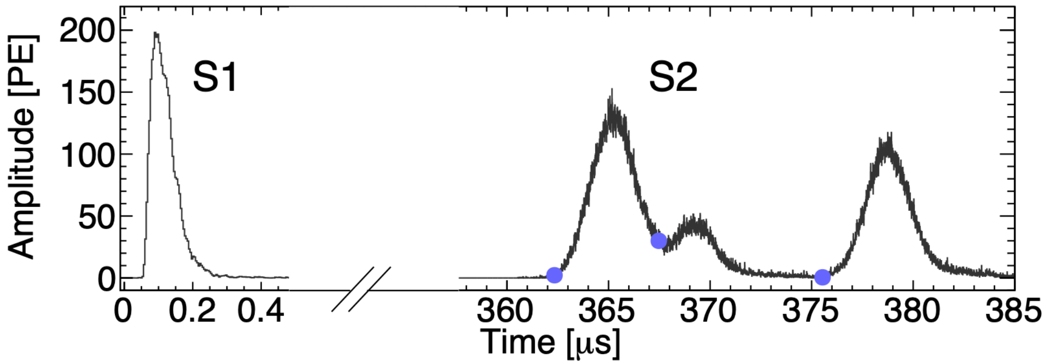

➢ Single-site (SS) selection:

- MeV-gamma event is mostly multi-site (MS) event, while the signal is mostly SS event;
- Identifying SS and MS with PMT waveforms;
- Validated with simulation and ^{232}Th calibration data;

Agreement in ROI is at 3.8% (Run0) and 3.7% (Run1), taken as systematic uncertainty later.

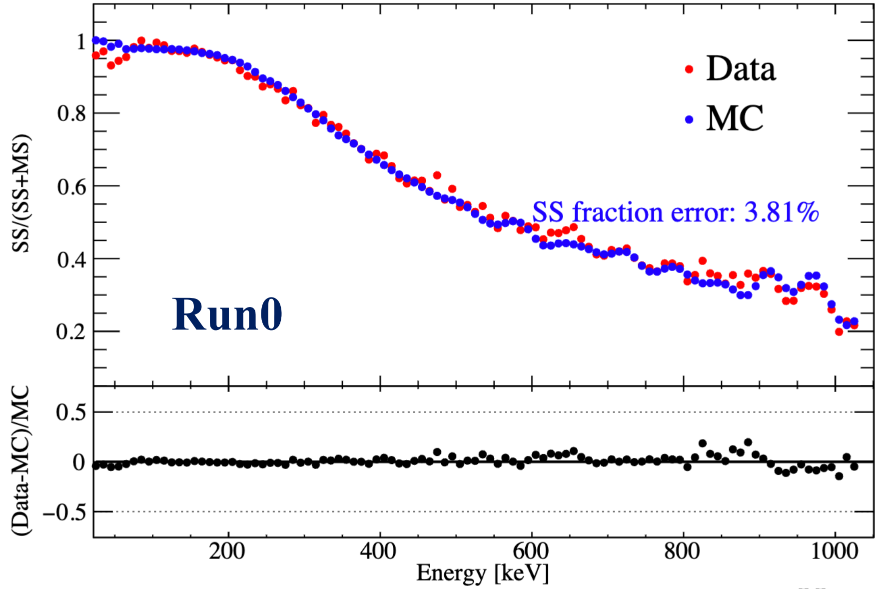

Background model

- **Biasing technology for material background**
  1. Split the sensitive volume;
  2. Record "bias_hit" and "bias_source";
  3. Generate the event by the "bias_source" from the previous run and increase the simulated numbers;
  4. Combine "bias_hit";
     - **"bias_hit":** Energy deposition;
     - **"bias_source":** The information of particles that touch the inner boundary.

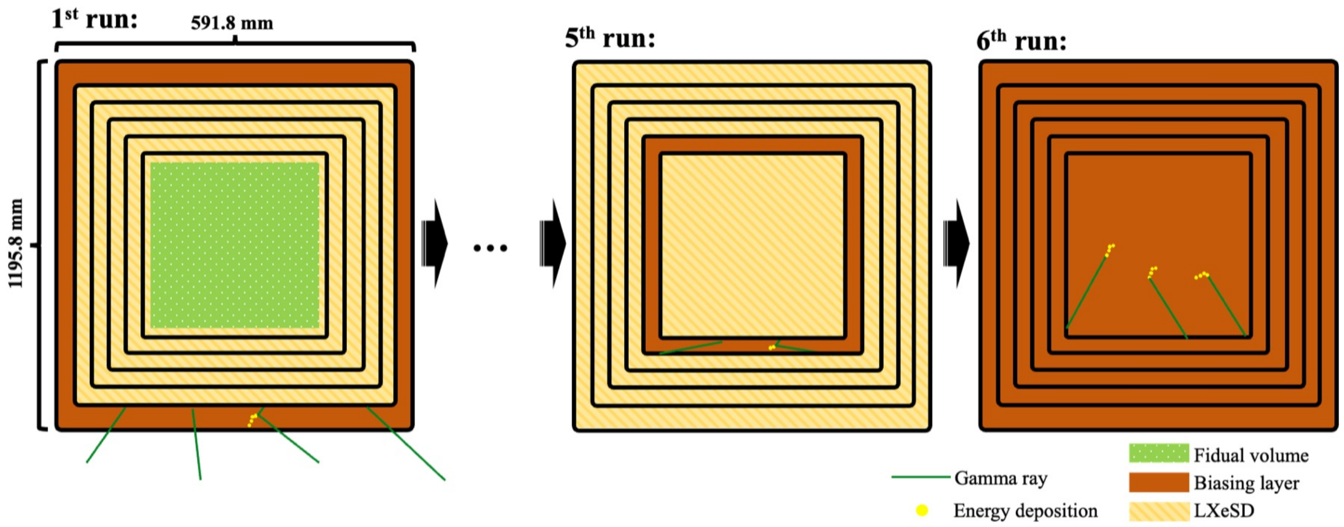

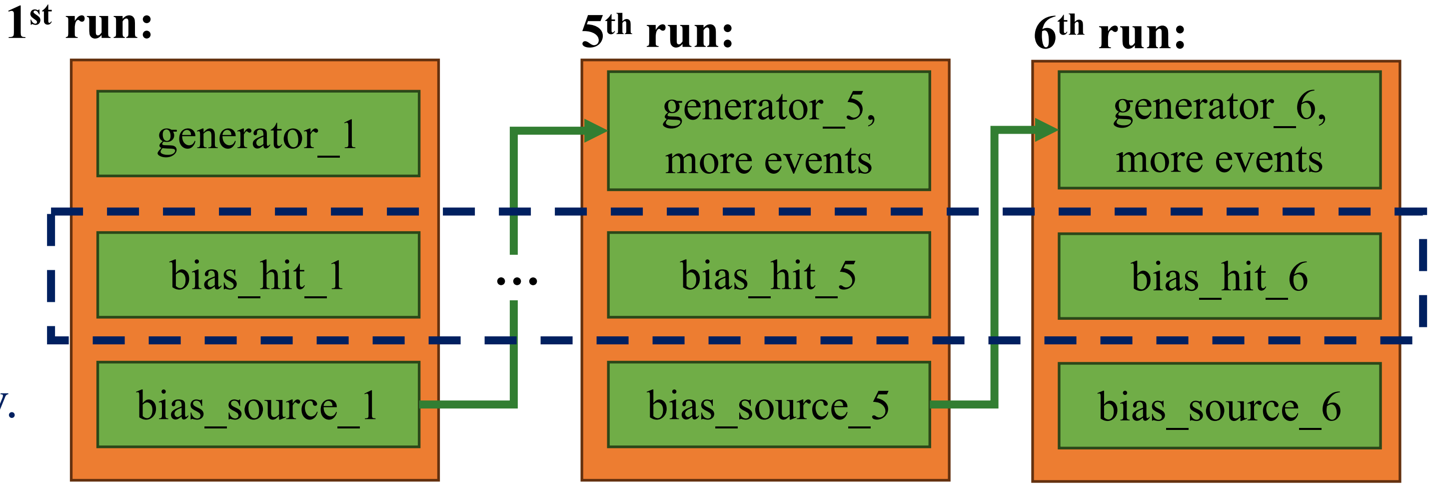

By reusing the results of previous layers, more statistics can be achieved in less time.

Background model

➢ **Detector materials:**

^{60}Co, ^{40}K, ^{232}Th, ^{238}U

- About 70 components from different locations.
- Expected radioactivates from the HPGe Station.
- Apply the **biasing** technology in the Monte-Carlo simulation.

Location		Isotope
Location 1	Location 2	
Inner vessel	Barrel Dome Bottom Dome Top FlangeB FlangeF	^{60}Co ^{40}K ^{232}Th ^{238}U ^{137}Cs
Outer vessel	Barrel Dome Bottom Dome Top FlangeB FlangeF	^{60}Co ^{40}K ^{232}Th ^{238}U ^{137}Cs
PMT	Body Bottom Body Top Base Bottom Base Top	^{60}Co ^{40}K ^{232}Th ^{238}U ^{137}Cs

Background-only Fit

- A background-only fit is performed prior to the signal fits, yielding a χ^2/NDF of 1.06.
- The data are consistent with the background-only model, with a p-value of 0.51. (^{85}Kr is pulled slightly upward by 1.5 σ)

Components	Expected ($\times 10^2$)	Fitted ($\times 10^2$)
^{232}Th	9.7 ± 5.8	12.7 ± 2.5
^{238}U	3.8 ± 2.8	6.6 ± 2.2
^{60}Co	5.8 ± 3.5	9.3 ± 3.0
^{40}K	4.5 ± 2.0	5.6 ± 1.9
^{85}Kr	19.0 ± 4.9	26.4 ± 2.3
^{214}Pb	float	352.9 ± 7.5
^{212}Pb	float	18.6 ± 2.5
^{136}Xe	352 ± 16	358.5 ± 9.1
^{124}Xe	1.37 ± 0.21	1.41 ± 0.13
^{125}Xe (Run0)	float	6.48 ± 0.83
^{125}I	0.66 ± 0.16	0.59 ± 0.13
^{133}Xe (Run0)	float	86.1 ± 2.2
164 keV (Run0)	414 ± 17	407.7 ± 6.4
164 keV (Run1)	float	4.67 ± 0.32
208 keV (Run0)	37.8 ± 1.3	37.88 ± 0.77
236 keV (Run0)	565 ± 66	560.8 ± 8.8
236 keV (Run1)	float	3.05 ± 0.32
380 keV (Run0)	24.3 ± 1.2	24.10 ± 0.66
408 keV (Run0)	87.9 ± 3.2	88.8 ± 1.6
$pp+^{7}$Be ν	2.22 ± 0.24	2.31 ± 0.23